Polym. Bull.
DOI 10.1007/s00289-016-1774-4

ORIGINAL PAPER

Influence of melt-mixing processing sequence on electrical conductivity of polyethylene/polypropylene blends filled with graphene

Ce Tu[1,2] · Kenji Nagata[2,3] · Shouke Yan[1]

Received: 7 April 2016 / Revised: 18 July 2016 / Accepted: 28 July 2016

Abstract In this paper, we produced composites of high-density polyethylene (PE)/polypropylene (PP) filled with graphene by melt compounding. Comparing composites produced in three processing sequences, we explored whether the sequence improved the composites' electrical conductivity. The (graphene/PE)/PP composite, prepared by simultaneous compounding, exhibited an electrical percolation threshold of 1.25 vol.%. In contrast, the (graphene/PP)/PE composite, prepared by blending the graphene with PP first and then blending the graphene/PP with PE, had a much lower electrical percolation threshold at less than 0.83 vol.%. At its percolation threshold, the (graphene/PP)/PE composite had a conductivity about two orders of magnitude higher than the (graphene/PE)/PP composite. We attribute this difference in conductivity to differences in the graphene distributions in the composites. In the (graphene/PE)/PP composite, the graphene sheets were selectively dispersed in the PE phase; in the (graphene/PP)/PE composite, some of the graphene was localized at the interface of the PE/PP blend. We also showed how the different processing sequences affected the composites' measured rheological and mechanical properties.

Keywords Graphene · Polymer blend · Processing sequence · Electrical percolation threshold · Selective localization

✉ Kenji Nagata
nagata.kenji@nitech.ac.jp

[1] State Key Laboratory of Chemical Resource Engineering, Beijing University of Chemical Technology, Beijing 100029, China

[2] Department of Materials Science and Engineering, Graduate School of Engineering, Nagoya Institute of Technology, Gokiso-cho, Showa-ku, Nagoya 466-8555, Japan

[3] Institute of Ceramics Research and Education, Nagoya Institute of Technology, Gokiso-cho, Showa-ku, Nagoya 466-8555, Japan

Journal : Small-ext 289 | Dispatch : 29-7-2016 | Pages : 16
Article No. : 1774 | LE | TYPESET
MS Code : POBU-D-16-00182 | CP | DISK

Introduction

Graphene has recently attracted significant attention from both the scientific and industrial communities because of its outstanding mechanical, electrical, and thermal properties [1–3]. Graphene can be dispersed in various polymer matrices to create a new class of polymeric composites with interesting properties [4, 5]. In particular, the high aspect ratio and electrical conductivity of graphene make it very effective at shielding electrical and electromagnetic interference when combined with insulating polymers [6–8]. Various reports have demonstrated the improved electrical properties of graphene-filled polyolefin [9], vinyl [10, 11], acrylic polymers [12, 13], polyester [14, 15], polyamide [9], polyurethane [16, 17], and epoxy [18] composites. This work has shown that conventional methods can produce inexpensive graphene-filled polymer composites as electronic materials.

When developing an electrically conductive composite, lowering its filler concentration helps to prevent the ductility, toughness, and processability of the matrix from deteriorating. Moreover, it appears much simpler to sufficiently decrease the filler concentration in a multiphase polymer blend than in a single-phase composite [19–23]. Of particular promise are composites whose conductive fillers are selectively localized either in one of the blend phases or at the interface of an immiscible co-continuous blend [20]. For example, Qi et al. [21] reported that selective localization of graphene in the polystyrene (PS) phase of PS/polylactic acid (PLA)/graphene composites produced a percolation threshold of 0.075 vol.%, while in PS/graphene composites the percolation threshold reached up to 0.33 vol.%. Mao et al. [24] revealed that composites of polystyrene (PS) and poly(methyl methacrylate) (PMMA) blends at a 50/50 PS/PMMA weight ratio, when filled with octadecylamine-functionalized graphene (GE-ODA), had a much lower percolation threshold (0.5 wt%) than did a PS/GE-ODA composite (2.0 wt%). These results indicate that selectively localizing fillers imparts an especially low electrical percolation threshold. Thus, understanding and controlling the localization of solid nanofillers in polymer blends is key to creating new electrically conductive composites [25].

Although selective localization of graphene has been very successful in polar polymers, such as poly(methyl methacrylate), polystyrene, polyethylene naphthalate, and polycarbonate [4, 21, 24], it has not been extensively explored in nonpolar polymers. One difficulty is dispersing polar nanofillers in polyolefin, which is nonpolar, and thus incompatible. To demonstrate this incompatibility, Steurer et al. [9] used transmission electron microscopy to show distinct stacks of many graphene layers in a polypropylene (PP) matrix. One of the most important commodity polyolefin thermoplastics is high-density polyethylene (PE) [26, 27]. Reinforcing it with rigid nanoparticles can improve its mechanical properties, and filling it with graphitic carbon can yield electrically and thermally conductive PE composites. Electrically conductive PE has potential for many applications, such as electromagnetic reflection, static charge dissipation, and as semiconductor layers in high-voltage cables [28, 29].

Journal : Small-ext 289 | Dispatch : 29-7-2016 | Pages : 16
Article No. : 1774 | LE | TYPESET
MS Code : POBU-D-16-00182 | CP | DISK

In this study, we selected PE and PP as binary matrices and prepared electrically conductive graphene-filled PE/PP composites by melt compounding. Melt compounding is a very attractive method for processing polymers because it is inexpensive and environmentally friendly, and it allows great flexibility in producing phase morphologies by selecting various polymers and in manufacturing high-performance polymer composites at the commercial scale. We investigated the selective localization of graphene in PE/PP composites using various compounding sequences of the graphene, PE and PP components; we succeeded in localizing the graphene at the PE/PP blend interface and lowering the electrical percolation threshold. Although selective localization of graphene in a single blend phase has been shown to reduce the percolation threshold in polymers, there seem to be few reports on selective localization of graphene at the blend interface in polymer composites. In this paper, we also systematically discuss how localization of graphene influences electrical, rheological, and mechanical properties.

Experimental

Materials

The composites were filled with pristine expanded graphite flakes (EC300, Ito Graphite Co., Ltd., Kuwana, Japan) with a mean size of 50 μm. Concentrated sulfuric acid (95–98 %), fuming nitric acid (85 %), hydrochloric acid (37 %), and potassium chlorate (98 %) were purchased from Nacalai Tesque Inc., Kyoto, Japan. The high-density PE (HI-Zex, 2100 J, Mitsui Chemicals Inc., Tokyo, Japan) had a density of 0.95 g/cm^3. The PP (Novatec-PP, MA3, Japan Polypropylene Co., Tokyo, Japan) had a density of 0.90 g/cm^3.

Preparation of graphene

Graphite oxide was prepared by oxidizing pristine graphite using the Staudenmaier method [30, 31]: First, expanded graphite flakes (5 g) were added to a vigorously stirred mixture of concentrated sulfuric acid (87.5 mL) and fuming nitric acid (45 mL). Potassium chlorate (55 g) was added over 15 min to the suspension, cooled by an ice-water bath. After reacting for 96 h, the reaction mixture was poured into 5 L of deionized water, stopping the reaction, and then filtered (Advantec No. 1 filter paper, Qualitative, Toyo Roshi Kaisha Ltd., Japan). The resultant graphite oxide was washed with 5 % hydrochloric acid until no sulfite ions were detected by a $BaCl_2$ test. The mixture was then washed with deionized water until the filtrate had a neutral pH when tested with test paper. The washed graphite oxide was centrifuged (Centrifuge 5220, Kubota Co., Ltd., Tokyo, Japan) and then freeze-dried (FD-5N, Tokyo Rikakikai Co., Ltd., Tokyo, Japan) for 72 h. Finally, the graphite oxide was thermally exfoliated in a muffle furnace (FT-101, Full-Tech Furnace Co., Ltd., Osaka, Japan) under a nitrogen atmosphere at ~1050 °C for ~60 s. This process produced sheets of thermally reduced graphene.

Journal : Small-ext 289 | Dispatch : 29-7-2016 | Pages : 16
Article No. : 1774 | LE | TYPESET
MS Code : POBU-D-16-00182 | CP | DISK

Preparation of graphene-filled PE/PP composites

Prior to compounding, the PE, PP, and graphene were dried at 50 °C under vacuum for 24 h. The graphene-filled PE/PP composites were prepared by melt compounding in a conical twin-screw extruder (HAAKE MiniLab, Thermo Fisher Scientific K.K., Yokohama, Japan) at 190 °C, rotating at 100 rpm for 15 min under N_2 purge. Based on previous results, we prepared the PE/PP blend with a composition of 60/40 wt% [32]. To study how the graphene location affected the morphology and electrical properties of the ternary composites, we made composites with three compounding sequences:

1. (*Graphene/PE*)/*PP* Graphene, PE, and PP were melt-compounded together for 15 min.
2. (*Graphene/PE*)/*PP* Graphene was compounded with PE for 10 min, and then the resulting graphene/PE masterbatch was blended with PP for 5 min.
3. (*Graphene/PP*)/*PE* Graphene was first compounded with PP for 5 min, and then the resulting graphene/PP blend was mixed with PE for 10 min.

To produce the test specimens, the extrudates were compression molded at 190 °C under 2.2 MPa. Note that we transformed the graphene content (ϕ) from a weight fraction (wt%) into a volume fraction (vol.%) by the following equation:

$$\phi = \frac{w/\rho_g}{w/\rho_g + (1-w)/\rho_b} \tag{1}$$

where ϕ is the volume fraction of graphene, w is the weight fraction of graphene, and ρ_g and ρ_b are the densities of graphene and the PE/PP blend matrix, respectively. We assume the density of graphene to be the theoretical value of 2.28 g/cm^3 [33, 34], and the calculated density of the PE/PP blend matrix (60/40 wt%) is 0.93 g/cm^3.

Characterization

The microstructures of graphene and the graphene-filled PE/PP composites were observed using transmission electron microscopy (TEM; JEM-z2500, JEOL Ltd., Tokyo, Japan) at an accelerating voltage of 200 kV. To prepare the TEM samples, the graphene sheets were dispersed in *N*,*N*-dimethyl-formamide, and this solution was dropped on a microscopy grid with an elastic carbon support film, while the PE/PP composites were cryogenically cut with a diamond knife at −140 °C to produce ultrathin sections (<80 nm). The thickness and lateral dimensions of the graphene were assessed using atomic force microscopy (AFM; Multimode 8, Nanoscope V, Bruker Instruments Inc., Germany) in tapping mode. These AFM samples were prepared by coating silicon substrates with the graphene/*N*,*N*-dimethyl-formamide suspensions. Field emission scanning electron microscopy (FE-SEM; JSM-7001F, JEOL, USA) was conducted at 15 kV. Before fracturing, the samples were immersed in liquid nitrogen and then sputtered with a thin layer of platinum using

Journal : Small-ext 289 | Dispatch : 29-7-2016 | Pages : 16
Article No. : 1774 | LE | TYPESET
MS Code : POBU-D-16-00182 | CP | DISK

an Auto Fine Coater (JEC-3000FC, JEOL). The rheological properties of the pure and composite samples were studied with a rheometer (VAR-50, Jasco Co., Tokyo, Japan) using a parallel-plate geometry with 25-mm-diameter plates at 190 °C under a nitrogen atmosphere. These measurements were performed in dynamic mode with the gap set to 0.7 mm. A frequency sweep was then performed from 0.01 to 90 rad/s.

Mechanical properties were measured using a tensile tester (Tensilon UTM-4-100, Toyo Baldwin Co., Ltd.). Specimens with dimensions of $20 \times 5 \times 0.5$ mm^3 were tested at a strain rate of 2 mm/min. The volume resistivity was tested with a two-point probe array (Advantest R8340A Ultra High Resistance Meter, Advantest Co., Tokyo, Japan) using an input voltage of 10 V. These specimens had a diameter of 50 mm and a thickness of 0.5 mm. To reduce the contact resistance between the samples and measuring electrodes, the samples were painted with conductive silver paste. All conductivity measurements were performed at ambient temperature.

Results and discussion

Graphene sheets

Figure 1a shows a TEM micrograph of graphene at low magnification. The transparent graphene sheet had a wrinkled surface, which would improve its interactions with the polymer matrix and facilitate its uniform dispersion [35]. The AFM image (Fig. 1b) also shows the wrinkled structure of the graphene, which had

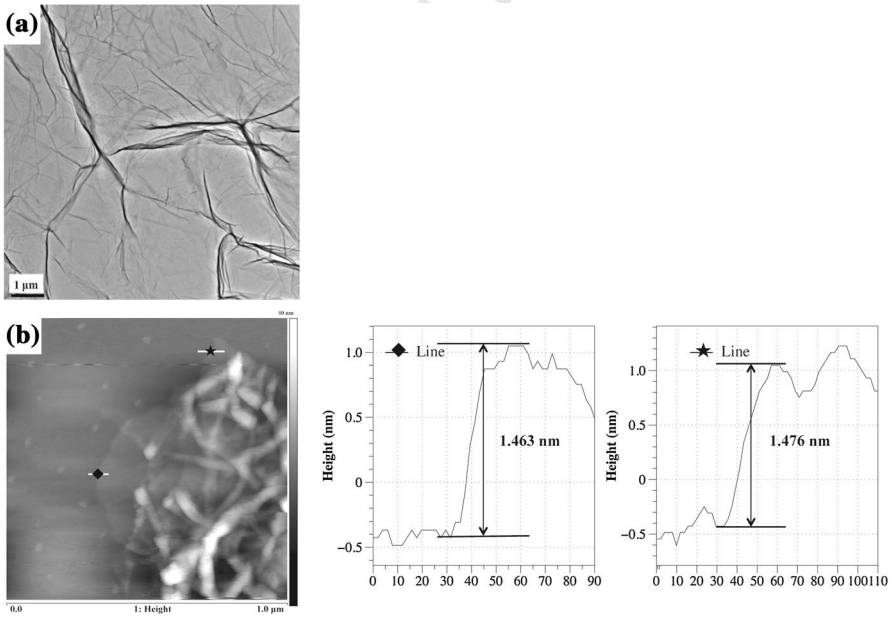

Fig. 1 **a** Transmission electron micrographs of the produced graphene with a wrinkled surface and **b** atomic force microscopy analysis of graphene sheets on the Si substrate

Journal : Small-ext 289 | Dispatch : 29-7-2016 | Pages : 16
Article No. : 1774 | LE | TYPESET
MS Code : POBU-D-16-00182 | CP | DISK

an average thickness of ~1.4 nm. Stankovich et al. [11] reported producing single layer graphene with a thickness of ~0.34 nm, so each platelet produced in our study may have three to five graphene layers.

Electrical conductivity and morphology

Figure 2 shows the electrical conductivity of the PE/PP (60/40) composites produced by various processing sequences as a function of graphene content. Adding the graphene greatly increased the electrical conductivity of all blends. With added graphene, the (graphene/PE)/PP composites rapidly transitioned from insulating to conducting behavior, with a percolation threshold smaller than 3 wt% (1.25 vol.%), implying that an interconnected graphene network formed in the composites, facilitating electron transport. This threshold is much lower than the thresholds of the melt-compounded graphene-filled single-PE composites (2.98 vol.%) and is almost equal to the thresholds of the solution-blended graphene/PE composites [36].

This low percolation threshold (1.25 vol.%) can be explained by selective localization of graphene in the (graphene/PE)/PP composites. The TEM micrographs in Fig. 3 show typical two-phase structures, whose dark and light parts correspond to the PE and PP phases, respectively.

In the (graphene/PE)/PP composite—in which the graphene, PE, and PP were compounded simultaneously—the graphene sheets were selectively dispersed in the PE phase, rather than in the PP phase, as shown in Fig. 3a. This selective localization is mainly caused by a difference in interfacial tension between the graphene and the two polymer components [37]. In binary blends, the localization behavior of fillers is dominated by interfacial effects and thermodynamic driving forces. Thus, one effective way to indicate the thermodynamic preference of

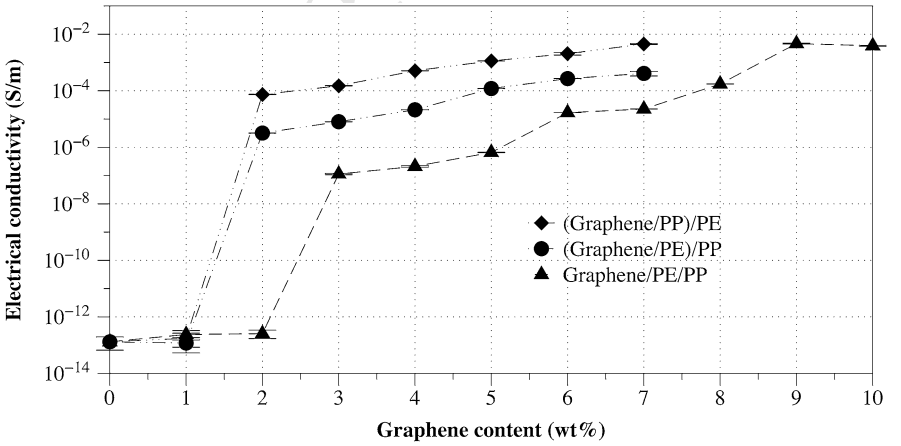

Fig. 2 Electrical conductivity of polyethylene (PE)/polypropylene (PP) (60/40 %) composites filled with graphene, produced with different processing sequences, as a function of graphene content

Journal : Small-ext 289 | Dispatch : 29-7-2016 | Pages : 16
Article No. : 1774 | LE | TYPESET
MS Code : POBU-D-16-00182 | CP | DISK

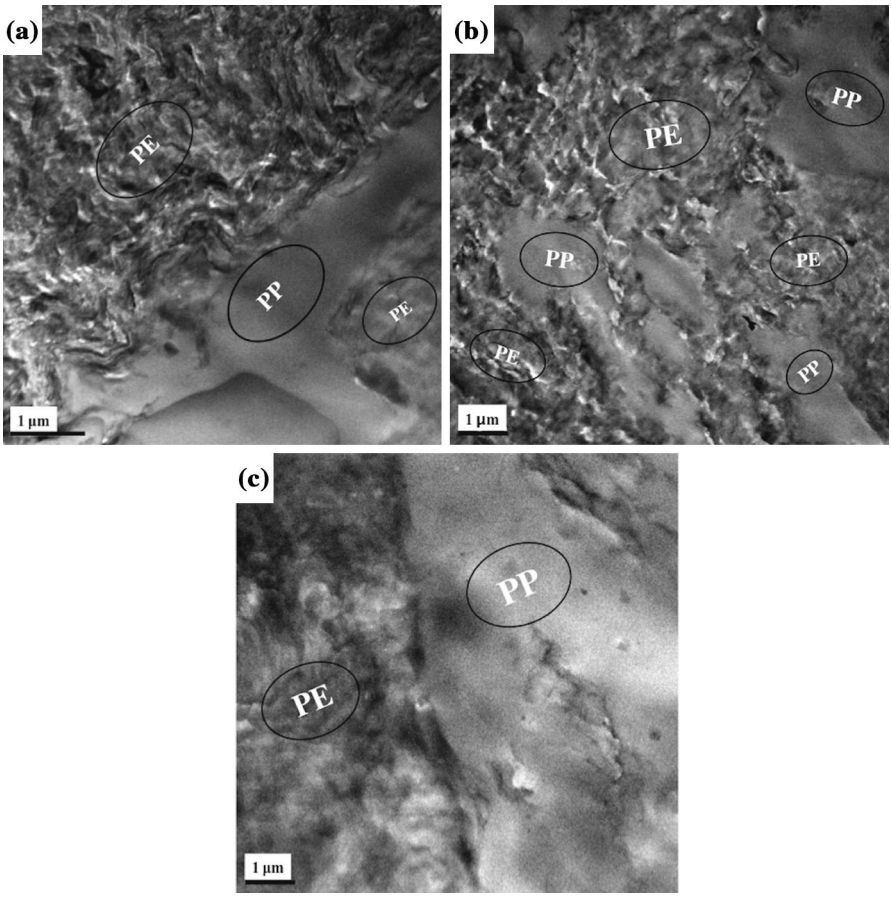

Fig. 3 Transmission electron micrographs of polyethylene (PE)/polypropylene (PP) (60/40 %) composites filled with 7 wt% graphene, prepared in three different sequences: **a** (graphene/PE)/PP, **b** (graphene/PE)/PP, and **c** (graphene/PP)/PE

graphene localization in PE/PP blends is by the wetting coefficient ω_a adapted by Sumita et al. [38] from Young's equation [39] (2):

$$\omega_a = \frac{\gamma_{\text{graphene/PE}} - \gamma_{\text{graphene/PP}}}{\gamma_{\text{PE/PP}}} \tag{2}$$

where $\gamma_{\text{graphene/PE}}$ represents the interfacial tension between graphene and PE, $\gamma_{\text{graphene/PP}}$ represents the interfacial tension between graphene and PP, and $\gamma_{\text{PE/PP}}$ represents the interfacial tension between PE and PP. The wetting coefficient ω_a is a simple mathematical description of the thermodynamic tendency of grapheme dispersion in immiscible PE/PP blends. When ω_a is smaller than -1, the graphene disperses within the PE phase; when ω_a is larger than 1, the graphene disperses within the PP phase; and when ω_a is between -1 and 1, the graphene becomes preferentially located at the PE/PP blend interface.

Journal : Small-ext 289 | Dispatch : 29-7-2016 | Pages : 16
Article No. : 1774 | LE | TYPESET
MS Code : POBU-D-16-00182 | CP | DISK

To calculate using Young's equation, the interfacial tensions must be calculated from surface tensions, following the Wu's harmonic mean average equation [40] (3):

$$\gamma_{1/2} = \gamma_1 + \gamma_2 - 4\left(\frac{\gamma_1^d \gamma_2^d}{\gamma_1^d + \gamma_2^d} + \frac{\gamma_1^p \gamma_2^p}{\gamma_1^p + \gamma_2^p}\right) \quad (3)$$

where γ_x in the numerator describes the surface tensions of the two components, equal to the sum of the dispersion γ^d and polar γ^p parts of the surface tensions.

The surface tensions γ_x of each component at 190 °C were taken from the literature [38, 41] and are listed in Table 1. Note that the surface tension of graphene is reported to be constant at various temperatures [41]. Using these values, we calculated the interfacial tension $\gamma_{1/2}$ and wetting coefficient ω_a, as listed in Table 2. Our calculated wetting coefficient is −2.88, indicating that the graphene sheets should be selectively located in the PE phase because the PE matrix has a lower interfacial tension with the graphene surface than does the PP matrix. These results agree with our TEM results; furthermore, this selective localization of graphene sheets in the PE phase and the volume-exclusion effect of PP in the composite produce a networked structure at a lower graphene content, which significantly reduces the percolation threshold of the composite [19].

As mentioned above, the thermodynamic driving force for grapheme localization is generated by the difference in interfacial tension, causing the graphene sheets to transfer from the PP phase, in which it was first mixed to the PE phase; this driving force causes the graphene to localize differently when the composite is processed in different sequences.

To further investigate how the processing sequence influenced the graphene localization and the composites' phase morphology and electrical properties, we adopted two other mixing sequences: (graphene/PE)/PP and (graphene/PP)/PE. The

Table 1 Surface tensions of PE, PP, and graphene (190 °C)

Sample	Surface tension (mN/m)			References
	Total (γ_x)	Dispersion part (γ^d)	Polar part (γ^p)	
PE	25.9	25.9	0	[38]
PP	20.2	19.8	0.4	[38]
Graphene	40.8	40.4	0.4	[41]

Table 2 Interfacial tensions and wetting coefficient of (graphene/PE)/PP composites

System	Possible pairs	Interfacial tension $\gamma_{A/B}$ (mN/m)	Wetting coefficient ω_a
(Graphene/PE)/PP	Graphene/PE	3.57	−2.88
	Graphene/PP	7.05	
	PE/PP	1.21	

Journal : Small-ext 289 | Dispatch : 29-7-2016 | Pages : 16
Article No. : 1774 | LE | TYPESET
MS Code : POBU-D-16-00182 | CP | DISK

processing sequence greatly affected the conductivity of the composites, as shown in Fig. 2. Mixing the graphene first with PE and then with the PP—producing the (graphene/PE)/PP composites—clearly improved the composite's conductivity and lowered its percolation threshold to less than 2 wt% (0.83 vol.%). At a graphene loading of 1.25 vol.%, the conductivity of the (graphene/PE)/PP composite could reach $\sim 8.04 \times 10^{-6}$ S/m. Achieving the same conductivity in the (graphene/PE)/PP composite would require 2.41 vol.% graphene.

For the (graphene/PE)/PP composite (Fig. 3b), almost all of the graphene sheets is preferentially localized in the PE matrix, and there are no graphene sheets in the white PP phase. The morphology of the PE phase was, however, separated into a net-like structure by the PP phase, making its continuous PE phase much thinner than that in the (graphene/PE)/PP composite. This morphology may improve the volume-exclusion effect of PP in the (graphene/PE)/PP composite, helping to develop the conductive network at the same graphene loading, increasing the conductivity and decreasing the graphene percolation threshold [42–44]. The volume-exclusion effect has applied well to polymer blends with graphene, such as polyamide 6/POE-*g*-MA/graphene composites [42], polyvinyl alcohol/carboxymethyl cellulose/graphene composites [43], polyamide 6/acrylonitrile–butadiene–styrene/graphene composites [44].

The greatest increase in conductivity came from mixing the graphene first with PP and then with PE, producing the (graphene/PP)/PE composites. In these composites, increasing their graphene content from 0.42 to 2.08 vol.% rapidly increased their electrical conductivity from $\sim 1.75 \times 10^{-13}$ to $\sim 1 \times 10^{-3}$ S/m. The 0.83-vol.% graphene-filled (graphene/PP)/PE composite showed an electrical conductivity of $\sim 7.35 \times 10^{-5}$ S/m. In contrast, the (graphene/PE)/PP composite with the same graphene content showed a conductivity of only $\sim 3.18 \times 10^{-6}$ S/m, more than an order of magnitude lower. Thus, the (graphene/PP)/PE composite had a lower percolation threshold than the (graphene/PE)/PP composite. In the (graphene/PP)/PE composite shown in Fig. 3c, in which graphene sheets are randomly dispersed in PE and PP, most sheets dispersed in the PE phase, with a small part dispersed in the PP phase. Some of the graphene was clearly localized at the interface of the PE/PP blends, and such morphology is very promising for developing an electrically conductive network at a relatively low filler concentration [4], which enabled the rather low percolation threshold of the (graphene/PP)/PE composites.

As shown in Fig. 4, because the graphene was first mixed with the PP phase, which is less thermodynamically favorable than the PE phase, the graphene sheets would migrate from the PP phase to the PE phase during the second mixing step: mixing the (graphene/PP) masterbatch with PE [39]. Some of the graphene sheets penetrated into the PE phase, while some approached their equilibrium position at the blend interface; this behavior caused some of graphene sheets to localize at the PE/PP interface, which is likely the ideal pattern for decreasing the electrical percolation threshold and improving the electrical conductivity.

The differences in phase structures and graphene localizations were confirmed by FE-SEM, as shown in Fig. 5. This figure shows the fractured surfaces of the PE/PP composites filled with 7 wt% graphene prepared in the three different processing

Journal : Small-ext 289 | Dispatch : 29-7-2016 | Pages : 16
Article No. : 1774 | LE | TYPESET
MS Code : POBU-D-16-00182 | CP | DISK

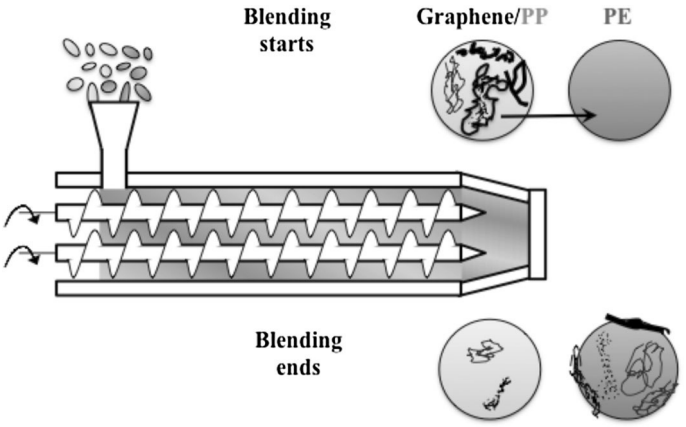

Fig. 4 Localization of graphene sheets from the polypropylene (PP) phase to the polyethylene (PE) phase during melt blending, as well as the graphene sheets located at the PE/PP blend interface in the (graphene/PP)/PE composite

sequences; the rough and smooth parts are the PE and PP phases, respectively, because the PE phase contains graphene. In the (graphene/PE)/PP composite (Fig. 5a), the PE matrix is a continuous phase, owing to its higher content (60 wt%). This image also reveals that the PP matrix had a smooth topology, indicating that it contained few graphene sheets. In the (graphene/PE)/PP composite (Fig. 5b), the PE matrix was similarly continuous and rough, but it formed a net-like structure, leading the continuous PE phase to be much thinner than that in the (graphene/PE)/PP composite; these results agree with our TEM results (Fig. 3a, b). In contrast, the (graphene/PP)/PE composite (Fig. 5c) exhibited a different morphology from the (graphene/PE)/PP and (graphene/PE)/PP composites: its PP phase was rougher (left part in Fig. 5c), possibly because a small portion of graphene was dispersed in the PP phase. The interface of the PE/PP blend was rough, confirming that the graphene was indeed located there.

The effect of compounding sequence on rheological and mechanical properties

The rheology of polymer composites appears to be very sensitive to the presence of filler networks, making rheometry one of the best methods to detect them [45]. For example, a characteristic low frequency plateau of the storage modulus G' appears when fillers form a percolated network [46].

Figure 6a shows the variation of storage modulus G' as a function of frequency ω in pure PE/PP and the graphene-filled PE/PP composites prepared with the three compounding sequences. The selected contents of graphene are 2 and 7 wt%; composites with other graphene contents are not shown here for ease of reading. In all of the composites, the storage modulus G' gradually increased with increasing graphene content, and the slope of the $G' - \omega$ curve began to decrease throughout the test range.

Journal : Small-ext 289 | Dispatch : 29-7-2016 | Pages : 16
Article No. : 1774 | LE | TYPESET
MS Code : POBU-D-16-00182 | CP | DISK

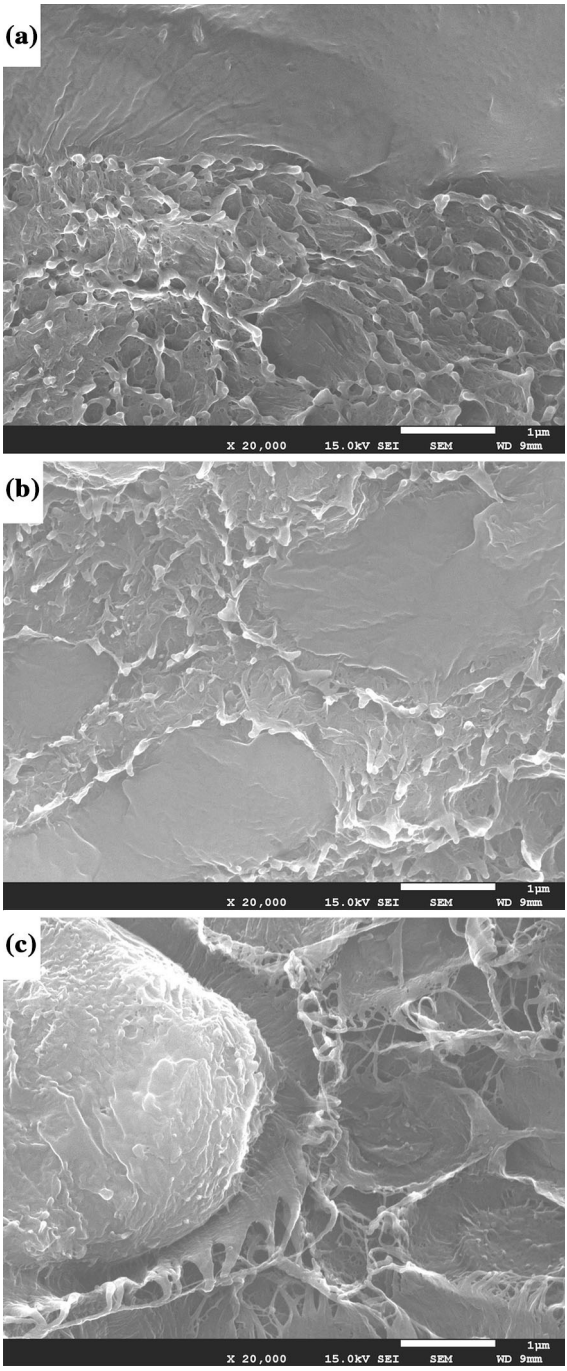

Fig. 5 Field-emission scanning electron micrographs of polyethylene (PE)/polypropylene (PP) (60/40 %) composites filled with 7 wt% graphene, prepared in three different sequences: **a** (graphene/PE)/PP; **b** (graphene/PE)/PP; and **c** (graphene/PP)/PE

Journal : **Small-ext 289** Dispatch : **29-7-2016** Pages : **16**
Article No. : **1774** □ LE □ TYPESET
MS Code : **POBU-D-16-00182** ☑ CP ☑ DISK

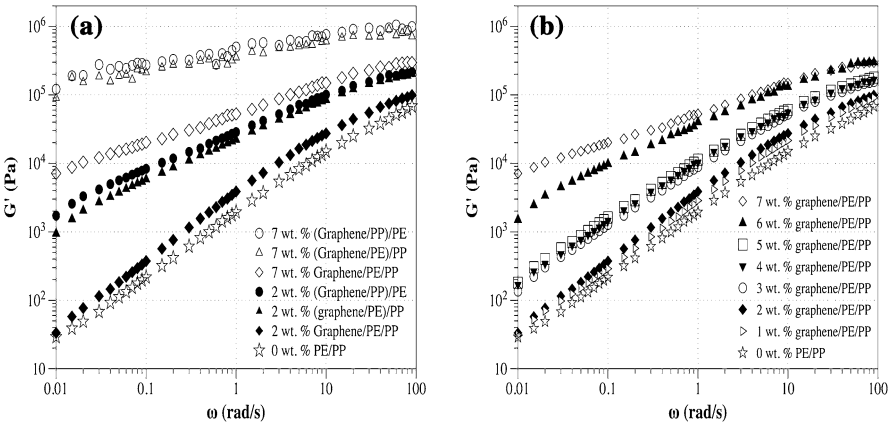

Fig. 6 Frequency dependence of the storage modulus G' of polyethylene (PE)/polypropylene (PP) (60/40 %) composites and graphene-filled PE/PP composites, **a** prepared in three different sequences: (graphene/PE)/PP, (graphene/PE)/PP, and (graphene/PP)/PE; and in **b** (graphene/PE)/PP composites with various graphene contents

This decrease in slope indicates that the composites gradually showed solid-like behavior, which comes about from the formation and development of the graphene networks [47]. At a graphene content of 2 wt%, both the (graphene/PP)/PE and (graphene/PE)/PP composites showed a much greater increase in G' at low frequency than did the (graphene/PE)/PP composite, which suggests that a percolated network formed in the (graphene/PP)/PE and (graphene/PE)/PP [47]. For the (graphene/PE)/PP composites, however, the first pronounced increase in G' at low frequency appeared at a graphene content of 3 wt% (Fig. 6b). Overall, the percolation thresholds of the rheological properties agree well with the percolation thresholds of the electrical properties shown in Fig. 2.

Note that at an equal graphene content (2 or 7 wt%), the (graphene/PP)/PE composites usually exhibited a slightly higher storage modulus than the (graphene/PE)/PP composites, whereas the (graphene/PE)/PP composites showed the lowest storage modulus. This result suggests that the (graphene/PP)/PE composite formed a more-developed conductive network at the same graphene loading. This trend in the composites' rheological properties agrees well with their electrical properties; the composites had the following order of electrical conductivity, from highest to lowest: (graphene/PP)/PE, (graphene/PE)/PP, and (graphene/PE)/PP.

A significant benefit of adding graphene is that it can enhance the mechanical properties of polymer matrices. Figure 7 shows stress–strain curves for the different composites, while Table 3 gives specific data for the Young's modulus (E), tensile strength (σ), and elongation at break (ε). The pure PE/PP composite had worse mechanical properties than the pure PE and PP polymers (PE: $E = 0.9$ GPa, $\sigma = 21$ MPa, and $\varepsilon = 370$ %; PP: $E = 1.6$ GPa, $\sigma = 35$ MPa, and $\varepsilon = 100$ %), especially for elongation, which is likely caused mainly by the lower miscibility between PE and PP [39, 40]; that is, the interface of the PE/PP composites were their primary mechanical defects. The graphene-filled composites with different

Journal : Small-ext 289 | Dispatch : 29-7-2016 | Pages : 16
Article No. : 1774 | LE | TYPESET
MS Code : POBU-D-16-00182 | CP | DISK

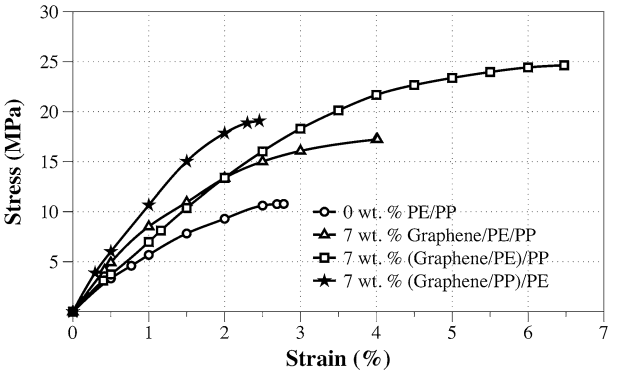

Fig. 7 Stress–strain *curves* of polyethylene (PE)/polypropylene (PP) (60/40 %) composites and 7 wt% graphene-filled PE/PP composites, prepared in three different sequences: (graphene/PE)/PP, (graphene/PE)/PP, and (graphene/PP)/PE

Table 3 Mechanical properties of graphene-filled PE/PP (60/40 %) composites

	0 wt% PE/PP	7 wt% (Graphene/PE)/PP	7 wt% (Graphene/PE)/PP	7 wt% (Graphene/PP)/PE
Young's modulus, E (GPa)	0.62 ± 0.02	0.97 ± 0.36	0.69 ± 0.13	1.29 ± 0.14
Tensile strength, σ (MPa)	10.8 ± 0.7	17.2 ± 3.7	24.6 ± 2.2	19.1 ± 2.4
Elongation at break, ε (%)	2.8 ± 0.1	4.0 ± 1.0	6.5 ± 0.8	2.4 ± 0.5

compounding sequences had different mechanical properties, even at the same graphene concentration. With added graphene, all of the composites increased in Young's modulus and tensile strength compared with the pure PE/PP composite, implying that the graphene actually confined the chains in their entanglements.

The Young's modulus increased most in the (graphene/PP)/PE composite, 1.29 GPa, which could have come from the graphene randomly dispersed in the PE and PP phases, allowing it to strengthen the composite more effectively before reaching its breaking point. On the other hand, because some graphene sheets were located at the PE/PP interface, the defects at the interface became large, lessening the elongation to 2.4 %. In the (graphene/PE)/PP composite, the net-like structure of the PE phase may have improved the volume-exclusion effect of the PP phase, reducing defects at the interface and increasing the tensile strength (to 24.6 MPa) and elongation (to 6.5 %). However, the difference in thermodynamic immiscibility between the original PE and PP phases greatly hinders the mechanical properties of the PE/PP composites, especially in elongation, so future work should look to improve the toughness of PE/PP blends.

Journal : Small-ext 289 | Dispatch : 29-7-2016 | Pages : 16
Article No. : 1774 | LE | TYPESET
MS Code : POBU-D-16-00182 | CP | DISK

Conclusion

Adding graphene sheets to PE/PP composites prepared by melt compounding improved their electrical conductivity. By varying the processing sequence of the graphene, PE, and PP components, we changed the localization of graphene in these composites, which changed their measured electrical conductivity. The composites had electrical conductivity in the following order, from highest to lowest: (graphene/PP)/PE, (graphene/PE)/PP, and (graphene/PE)/PP. In the (graphene/PP)/PE composite, mixing the graphene/PP first and then melt-mixing the graphene/PP with PE encouraged the graphene sheets to localize at the PE/PP blend interface; this structure is likely ideal for decreasing the percolation threshold; we produced a percolation threshold lower than 0.83 vol.%. The measured rheological properties of the composites agree with their measured electrical properties, confirming that the (graphene/PP)/PE composite formed a better graphene network than the other composites with the same graphene loading. The results of mechanical measurements imply that the brittleness of PE/PP blends remains an issue.

Acknowledgments We gratefully acknowledge the financial support of the National Natural Science Foundation of China (Grant Nos. 51221002 and 21174014). We also thank the Instrument and Research Technology Center at Nagoya Institute of Technology for AFM, TEM, and FE-SEM analyses.

References

1. Terrones M, Martín O, Gonzalez M, Pozuelo J, Serrano B, Cabanelas JC, Vega-Diaz SM, Baselga J (2011) Interphases in graphene polymer-based nanocomposites: achievements and challenges. Adv Mater 23:5302–5310
2. Geim AK (2009) Graphene: status and prospects. Science 324:1530–1534
3. Geim AK, Novoselov KS (2007) The rise of graphene. Nat Mater 6:183–191
4. Kim H, Abdala AA, Macosko CW (2010) Graphene/polymer nanocomposites. Macromolecules 43:6515–6530
5. Yang J, Lin Y, Wang J, Lai M, Li J, Liu J, Tong X, Cheng H (2005) Morphology, thermal stability, and dynamic mechanical properties of atactic polypropylene/carbon nanotube composites. J Appl Polym Sci 98:1087–1091
6. Kim H, Kobayashi S, AbdurRahim MA, Zhang MJ, Khusainova A, Hillmyer MA, Abdala AA, Macosko CW (2011) Graphene/polyethylene nanocomposites: effect of polyethylene functionalization and blending Methods. Polymer 52:1837–1846
7. Ling JQ, Zhai WT, Feng WW, Shen B, Zhang JF, Zheng WG (2013) Facile preparation of lightweight microcellular polyetherimide/graphene composite foams for electromagnetic interference shielding. ACS Appl Mater Interfaces 5:2677–2684
8. Zhang HB, Yan Q, Zheng WG, He Z, Yu ZZ (2011) Tough graphene—polymer microcellular foams for electromagnetic interference shielding. ACS Appl Mater Interfaces 3:918–924
9. Steurer P, Wissert R, Thomann R, Muelhauptv R (2009) Functionalized graphenes and thermoplastic nanocomposites based upon expanded graphite oxide. Macromol Rapid Commun 30:316–327
10. Achaby ME, Arrakhiz FZ, Vaudreuil S, Essassi EM, Qaiss A, Bousmina M (2013) Preparation and characterization of melt-blended graphene nanosheets–poly(vinylidene fluoride) nanocomposites with enhanced properties. J Appl Polym Sci 127:4697–4707
11. Stankovich S, Dikin DA, Dommett GHB, Kohlhaas KM, Zimney EJ, Stach EA, Piner RD, Nguyen ST, Ruoff RS (2006) Graphene-based composite materials. Nature 442:282–286
12. Jang JY, Kim MS, Jeong HM, Shin CM (2009) Graphite oxide/poly(methyl methacrylate) nanocomposites prepared by a novel method utilizing macroazoinitiator. Compos Sci Technol 69:186–191

Journal : Small-ext 289 | Dispatch : 29-7-2016 | Pages : 16
Article No. : 1774 | LE | TYPESET
MS Code : POBU-D-16-00182 | CP | DISK

13. Wang WP, Pan CY (2004) preparation and characterization of poly(methyl methacrylate)-intercalated graphite oxide/poly(methyl methacrylate) nanocomposite. Polym Eng Sci 44:2335–2339
14. Kim H, Macosko CW (2009) Processing-property relationships of polycarbonate/graphene composites. Polymer 50:3797–3809
15. Kim H, Macosko CW (2008) Morphology and properties of polyester/exfoliated graphite nanocomposites. Macromolecules 41:3317–3327
16. Kim H, Miura Y, Macosko CW (2010) Graphene/polyurethane nanocomposites for improved gas barrier and electrical conductivity. Chem Mater 22:3441–3450
17. Raghu AV, Lee YR, Jeong HM, Shin CM (2008) Preparation and physical properties of waterborne polyurethane/functionalized graphene sheet nanocomposites. Macromol Chem Phys 209:2487–2493
18. Liang J, Wang Y, Huang Y, Ma Y, Liu Z, Cai J, Zhang C, Gao H, Chen Y (2009) Electromagnetic interference shielding of graphene/epoxy composites. Carbon 47:922–925
19. Gubbels F, Jerome R, Teyssie P, Vanlathem E, Deltour R, Calderone A, Parente V, Bredas JL (1994) Selective localization of carbon black in immiscible polymer blends: a useful tool to design electrical conductive composites. Macromolecules 27:1972–1974
20. Gubbels F, Blacher S, Vanlathem E, Jerome R, Deltour R, Brouers F, Teyssie P (1995) Design of electrical composites: determining the role of the morphology on the electrical properties of carbon black filled polymer blends. Macromolecules 28:1559–1566
21. Qi XY, Yan D, Jiang ZG, Cao YK, Yu ZZ, Yavari F, Koratkar N (2011) Enhanced electrical conductivity in polystyrene nanocomposites at ultra-low graphene content. ACS Appl Mater Interfaces 3:3130–3133
22. Thongruang W, Spontak RJ, Balik CM (2002) Bridged double percolation in conductive polymer composites: an electrical conductivity, morphology and mechanical property study. Polymer 43:3717–3725
23. Meincke O, Kaempfer D, Weickmann H, Friedrich C, Vathauer M, Warth H (2004) Mechanical properties and electrical conductivity of carbon-nanotube filled polyamide-6 and its blends with acrylonitrile/butadiene/styrene. Polymer 45:739–748
24. Mao C, Zhu YT, Jiang W (2012) Design of electrical conductive composites: tuning the morphology to improve the electrical properties of graphene filled immiscible polymer blends. ACS Appl Mater Interfaces 4:5281–5286
25. Wegrzyn M, Juan S, Benedito A, Gimenez E (2013) The influence of injection molding parameters on electrical properties of PC/ABS-MWCNT nanocomposites. J Appl Polym Sci 130:2152–2158
26. Linares A, Canalda JC, Cagiao ME, GarcIa-GutiErrez MC, Nogales A, Martin-Gullon I, Vera J, Ezquerra TA (2008) Broad-band electrical conductivity of high density polyethylene nanocomposites with carbon nanoadditives: multiwall carbon nanotubes and carbon nanofibers. Macromolecules 41:7090–7097
27. Moniruzzaman M, Winey KI (2006) Polymer nanocomposites containing carbon nanotubes. Macromolecules 39:5194–5205
28. Munson-McGee SH (1991) Estimation of the critical concentration in an anisotropic percolation. Phys Rev B 43:3331–3336
29. Zheng WG, Lu XH, Wong SC (2004) Electrical and mechanical properties of expanded graphite-reinforced high-density polyethylene. J Appl Polym Sci 91:2781–2788
30. Schniepp HC, Li JL, McAllister MJ, Sai H, Herrera-Alonso M, Adamson DH, Prud'homme RK, Car R, Saville DA, Aksay IA (2006) Functionalized single graphene sheets derived from splitting graphite oxide. J Phys Chem. B 110:8535–8539
31. McAllister MJ, Li JL, Adamson DH, Schniepp HC, Abdala AA, Liu J, Herrera-Alonso M, Milius DL, Car R, Prud'homme RK, Aksay IA (2007) Single sheet functionalized graphene by oxidation and thermal expansion of graphite. Chem Mater 19:4396–4404
32. Nagata K, Kimura Y, Takahashi K, Kinoshita T (2002) Localization of carbon black particles in polypropylene/polyethylene polymer blend and its electrical resistivity. Jpn J Polym Sci Technol 59:694–701
33. Grossiord N, Loos J, Koning CE (2005) Strategies for dispersing carbon nanotubes in highly viscous polymers. J Mater Chem 15:2349–2352
34. Kelly B (1981) Physics of graphite. In: Englewood NJ (ed). Applied Science Publishers, London, pp 267–361
35. Rafiee MA, Rafiee J, Wang Z, Song HH, Yu ZZ, Koratkar N (2009) Enhanced mechanical properties of nanocomposites at low graphene content. ACS Nano 3:3884–3890

Journal : Small-ext 289 | Dispatch : 29-7-2016 | Pages : 16
Article No. : 1774 | □ LE | □ TYPESET
MS Code : POBU-D-16-00182 | ☑ CP | ☑ DISK

36. Dua JH, Zhao L, Zeng Y, Zhang LL, Lia F, Liu PF, Liu C (2011) Comparison of electrical properties between multi-walled carbon nanotube and graphene nanosheet/high density polyethylene composites with a segregated network structure. Carbon 49:1094–1100
37. Goldel A, Marmur A, Kasaliwal GR, Potschke P, Heinrich G (2011) Shape-dependent localization of carbon nanotubes and carbon black in an immiscible polymer blend during melt mixing. Macromolecules 44:6094–6102
38. Sumita M, Sakata K, Asai S, Miyasaka K, Nakagawa H (1991) Dispersion of fillers and the electrical conductivity of polymer blends filled with carbon black. Polym Bull 25:265–271
39. Young T (1805) An essay on the cohesion of fluids. Philos Trans R Soc Lond 95:65–87
40. Wu S (1982) Polymer interface and adhesion. Marcel Dekker, New York
41. Shen Y, Zhang TT, Yang JH, Zhang N, Huang T, Wang Y (2016) Selective localization of reduced graphene oxides at the interface of PLA/EVA blend and its resultant electrical resistivity. Polym Compos. doi:10.1002/pc.23769
42. Yan D, Zhang HB, Jia Y, Hu J, Qi XY, Zhang Z, Yu ZZ (2012) Improved electrical conductivity of polyamide 12/graphene nanocomposites with maleated polyethylene-octene rubber prepared by melt compounding. ACS Appl Mater Interfaces 4:4740–4745
43. Guin JP, Chaudhari CV, Dubey KA, Bhardwaj YK, Varshney L (2015) Graphene reinforced radiation crosslinked polyvinyl alcohol/carboxymethyl cellulose nanocomposites for controlled drug release. Polym Compos. doi:10.1002/pc.23823
44. Bouhfid R, Arrakhiz FZ, Qaiss A (2016) Effect of graphene nanosheets on the mechanical, electrical, and rheological properties of polyamide 6/acrylonitrile–butadiene–styrene blends. Polym Compos 37:998–1006
45. Hyun YH, Lim ST, Choi HJ, Jhon MS (2001) Rheology of poly(ethylene oxide)/organoclay nanocomposites. Macromolecules 34:8084–8093
46. Zhu YT, Cardinaels R, Mewis J, Moldenaers P (2009) Rheological properties of PDMS/clay nanocomposites and their sensitivity to microstructure. Rheol Acta 48:1049–1058
47. Zhang QH, Fang F, Zhao X, Li YZ, Zhu MF, Chen DJ (2008) Use of dynamic rheological behavior to estimate the dispersion of carbon nanotubes in carbon nanotube/polymer composites. J Phys Chem B 112:12606–12611

Journal : **Small-ext 289**	Dispatch : **29-7-2016**	Pages : **16**
Article No. : **1774**	□ LE	□ TYPESET
MS Code : **POBU-D-16-00182**	☑ CP	☑ DISK